Title
ATTRACTIVE WELL OF He-He FROM He3-He DIFFERENTIAL ELASTIC SCATTERING MEASUREMENTS

Author
Burgmans, A.L.J.

Publication Date
1975-07-01

Submitted to Journal of Chemical Physics

LBL-4072
Preprint c.

ATTRACTIVE WELL OF He-He FROM He^3-He^4 DIFFERENTIAL ELASTIC SCATTERING MEASUREMENTS

A. L. J. Burgmans, J. M. Farrar, and Y. T. Lee

July 1975

Prepared for the U. S. Energy Research and Development Administration under Contract W-7405-ENG-48

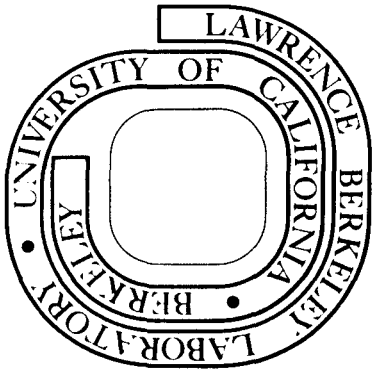

DISCLAIMER

ATTRACTIVE WELL OF He-He FROM He^3-He^4 DIFFERENTIAL ELASTIC SCATTERING MEASUREMENTS*

A. L. J. Burgmans,† J. M. Farrar and Y. T. Lee

Department of Chemistry and The James Franck Institute
The University of Chicago, Chicago, Illinois 60637

and

Department of Chemistry and Lawrence Berkeley Laboratory‡
University of California, Berkeley, California 94720

ABSTRACT

The elastic differential cross section for He^3-He^4 was measured at a relative collision energy of 0.799×10^{-14} erg, approximately five times the well depth. The data are fitted to a multiparameter potential form with $\epsilon/k = 10.57°K$ and $r_m = 2.97$ Å. Comparisons with recent experimental and theoretical helium potentials are made. No evidence for a significant isotope effect in the He^3-He^4 and He^4-He^4 interatomic potentials is found in this work.

I. INTRODUCTION

Among the homonuclear rare gas pairs, the interaction between two helium atoms has generated the most experimental and theoretical activity in recent years. Initial experimental work on corrections to the helium gas thermometer led to values of the second virial coefficient at low temperatures[1] which were interpreted using model potentials. The deBoer-Michels potential[2] of the Lennard-Jones (12-6) form resulted from such calculations and has enjoyed considerable success in fitting transport and virial coefficient data below 100°K. More recent bulk phenomena measurements,[3-6] particularly at extremely low and high temperatures have led to more refined potentials, exemplified by the Beck potential[7] which has been shown to fit many properties of gaseous helium over a wide temperature range.

Beginning with the high energy scattering measurements of Amdur et al[8] and the complementary calculations of Phillipson,[9] Gilbert and Wahl,[10] Matsumoto et al,[11] and other workers,[12] the nature of the short range repulsion has been developed and can be characterized as fairly well understood. Theoretical work has also provided a consistent picture of the long range interaction,[13] leaving the intermediate region of the attractive well as the focal point of many recent experimental and theoretical studies. Earlier work from this laboratory[14,15] employing the crossed molecular beam technique at very low energy has provided some information regarding the lower repulsive wall of the potential as well as the attractive minimum. The work of Scoles[16] employing the same technique has yielded consistent results for the low energy repulsion. Two recent measurements of the total elastic scattering cross section as

a function of collision energy have also provided keen insight into this region of the interatomic potential. Feltgen et al[17] have measured the velocity dependence of the He^4-He^4 total elastic scattering cross section and have resolved oscillatory structure arising from backward glories. These data provide information on the energy dependence of the s-wave phase shift and thus can be inverted to yield a portion of the interatomic potential,[18] the low energy repulsion up to 0.14 eV. Bennewitz et al[19,20] have reported two experiments which complement the results obtained by other workers. A He^4-He^4 total cross section measurement extending to lower energies than that of Feltgen et al yields a potential, the low energy repulsive wall of which is in excellent agreement with that of the latter work and with recent accurate *ab initio* calculations by Liu and McLean.[21] Additionally, these measurements yield a value of the attractive well depth of $\varepsilon/k = 10.3°K$, a few percent shallower than the 11.0°K value reported in an earlier communication from this laboratory.[15] The second experiment of Bennewitz et al was performed on He^3-He^3 and the well depth for this system was found to be 3.4% larger than for the He^4-He^4 case. Such a conclusion suggests that the Born-Oppenheimer (B.O.) separation of electronic and nuclear motion usually performed in calculations may not be valid when the strength of the interaction is a very small fraction of the total electronic energy of the system. Calculations in which adiabatic corrections are made to the B.O. approximation have been performed,[22] but a more complete treatment may be necessary. Additionally, the inclusion of intra-atomic correlation effects in *ab initio* calculations has been shown to be important in the well region but difficult to carry out correctly.[23,24] Nevertheless, the recent more extensive and more accurate calculation by Liu and McLean[21]

has brought the calculated attractive well of helium potential in closer agreement with experimental results.

Thus, while experimental and theoretical results seem to be converging toward a valid picture of the He-He interaction in the region of the attractive minimum, significant further progress is hampered from the theoretical front by the difficulty of complete treatment of the intra-atomic correlation energy contribution and possible breakdown of the Born Oppenheimer separation of nuclear and electronic coordinates. Experimentally, cross sections measured at the requisite low collision energies have little structure because of the small number of partial waves contributing to the scattering amplitude. In our earlier work, we have indicated that at a collision energy of $.799 \times 10^{-14}$ erg, only five partial waves have phase shifts > 0.05 rad, thereby limiting the information which can be extracted from the data. Since the He^4 nucleus is a spinless Boson, only even-ℓ waves contribute to the scattering amplitude; in the He^3-He^3 case, all ℓ's contribute with even- and odd-ℓ terms weighted differently in accordance with Fermi statistics appropriate to the He^3 nucleus. In the present work, we have measured the elastic differential cross section of He^3 scattered from He^4 at a collision energy of $.799 \times 10^{-14}$ erg with a twofold goal: 1) In this nonsymmetric case, the occurrence of both even- and odd-ℓ partial waves should effectively double the information content of the experiment and yield more structure and hence a less ambiguous potential form. 2) To attempt to discern an isotope effect between the He^3-He^4 and He^4-He^4 potentials.

II. EXPERIMENTAL

The crossed molecular beam technique described in the previous communications from this laboratory[14,15] was also employed here and hence no further discussion of the general experimental arrangement is found here. The low energy helium beams were formed by the usual isentropic expansion from a liquid-hydrogen cooled beam source, yielding a collision energy of $.799 \times 10^{-14}$ erg. The He^3 scattered intensity was recorded; because of the scarcity of the He^3 gas, the experiment was performed by counting the He^3 signal for 10 sec and periodically returning to an arbitrarily selected reference angle. Several angular scans were made; in spite of the very short counting time the low mass 3 background in the mass spectrometer made the statistics of such data points quite acceptable, with a standard deviation at the reference angle of 10° from the He^3 beam of ± 1%.

III. RESULTS

The experimental angular distribution is shown in Fig. 1. The data for the He^4-He^4 experiment from paper III are also shown for comparison. The noticeably improved signal to noise ratio for the present data is apparent, a reflection of the low mass 3 background in the detector (prior to this experiment). The effect of nuclear symmetry arising from cancellation of the odd-ℓ terms in the He^4-He^4 spinless Boson scattering amplitude is absent in the present data, as evidenced by the lack of a deep minimum in the cross section at $\Theta = 33°$.

The data were fitted in the usual way by assuming a multiparameter potential form and calculating center of mass (c.m.) differential cross sections at a set of energies to simulate the finite energy dispersion of

the beams. These c.m. cross sections are then transformed to the laboratory system in the standard manner and the finite angular acceptance of the detection system is accounted for by folding in the apparatus "resolution function". The radial Schrödinger equation is integrated via the Numerov algorithm to yield phase shifts as a function of angular momentum ℓ; for large ℓ phase shifts with $\eta_\ell < .05$, the Born approximation generates these numbers to a limit of 0.001 rad. The calculated phase shifts then yield the cross section via the Rayleigh-Faxen-Holtsmark partial wave expansion as follows:

$$\frac{d\sigma}{d\theta} = |f(\theta)|^2$$

$$f(\theta) = (2ik)^{-1} \sum_{\ell} (2\ell+1)[\exp(2i\eta_\ell - 1)]P_\ell(\cos\theta)$$

where $k = \hbar^{-1}\sqrt{2\mu E}$ and $P_\ell(\cos\theta)$ is the usual Legendre polynomial.

The parametric potential form chosen is the Exponential-Spline-Morse-Morse Spine-van der Waals (ESMMSV) piecewise function suggested in earlier work,[14] with the following form:

$$x = r/r_m$$

$$f(x) = V(r)/\epsilon$$

$$f(x) = Ae^{-\alpha(x-1)} \qquad x \leq x_1$$

$$= \exp\left[\left[a_1 + (x-x_1)\left\{a_2 + (x-x_2)[a_3 + (x-x_1)a_4]\right\}\right]\right] \qquad x_1 < x < x_2$$

$$= e^{-2\beta(x-1)} - 2e^{-\beta(x-1)} \qquad x_2 \leq x \leq 1$$

$$= e^{-2\beta'(x-1)} - 2e^{-\beta'(x-1)} \qquad 1 < x \leq x_3$$

$$= b_1 + (x - x_3)\left\{b_2 + (x - x_4)[b_3 + (x - x_3)b_4]\right\} \qquad x_3 < x < x_4$$

$$= -c_6 x^{-6} - c_8 x^{-8} - c_{10} x^{-10} \qquad x \geqslant x_4$$

$$c_n = C_n/(\varepsilon r_m^n)$$

The parameters which provide a best fit to the scattering data are listed here:

ε/k	= 10.57°K	a_4	= -362.002
r_m	= 2.97 Å	b_1	= -0.65000
β	= 6.475	b_2	= 1.4516
β'	= 5.964	b_3	= -4.02889
A	= 0.343	b_4	= 4.51927
α	= 15.058	x_1	= 0.70000
a_1	= 3.4469	x_2	= 0.84477
a_2	= -19.0218	x_3	= 1.15016
a_3	= -28.0670	x_4	= 1.50000

The long range force constants are given as follows:

$C_6 = 1.40 \times 10^{-12}$ erg Å^6 (ref. 13)

$C_8 = 3.78 \times 10^{-12}$ erg Å^8 (ref. 28)

$C_{10} = 13.7 \times 10^{-12}$ erg Å^{10} (ref. 26)

The short range exponential repulsion terms A and α differ from those used in our previous work. These values were chosen for the present work to constrain our potential to fit the repulsive potential derived

by Pauly from backward glory scattering data.[17] This portion of the potential is in agreement with that proposed by Bennewitz et al,[19] McLaughlin and Schaefer,[12] and Liu and McLean.[21]

The scattering data were fitted by varying four parameters and comparing calculated cross sections with the data. The parameters varied were ε, r_m, β, and β'. The different values for β and β' were necessary in order to join the repulsion smoothly to the exponential terms; the larger value of β was necessary to do this while maintaining a reasonable value of σ. A smaller value of β' was chosen to maintain the strength of the outer wall attraction as evidenced by the small angle scattering.

In order to provide a comparison among the recently proposed helium potentials, we have compared the potential derived in this work with *ab initio* calculations of Liu and McLean[21] (LM) and with the experimentally determined potential of Bennewitz et al,[19] denoted mLJ-D. For purposes of calculation we have fitted the LM potential to an analytic form which reproduces the calculated points to $\lesssim 1\%$. The depth and range parameters for this potential are given by $\varepsilon/k = 10.76°K$, $r_m = 2.963$ Å.

The mLJ-D form is a piecewise potential constructed by joining the Morse function repulsion of Bruch and McGee's MDD-2 potential[27] to the theoretical long range terms of Davison,[28] using Lennard-Jones (N,6) potentials to describe the well region:

$$
\begin{aligned}
V(r) &= \text{MDD-2} && r < 2.15 \text{ Å} \\
&= \text{LJ}(8.8,6) && 2.15 \text{ Å} \leq r \leq \sigma \\
&= \text{LJ}(14.5,6) && \sigma < r \leq 6.3 \text{ Å} \\
&= -c_6 r^{-6} - c_8 r^{-8} && r > 6.3 \text{ Å}
\end{aligned}
$$

$$\epsilon/k = 10.30°K$$

$$r_m = 2.979 \text{ Å}$$

$$\sigma = 2.685 \text{ Å}$$

These potentials are plotted in Fig. 2 along with the ESMSV-II potential of our earlier work. The similarities among the LM, mLJ-D, and present potentials are apparent,with the well depth of the latter intermediate between LM and mLJ-D.

In Fig. 3 we show calculated cross sections for the He^3-He^4 system performed with these potentials. Because of the small number of partial waves involved in the scattering, the cross sections do not show rainbow structure but rather only diffractive quantum oscillations. The primary differences among the cross sections computed with these potentials appear at small angles where the experimental points are determined with greatest precision. In order to show more clearly the features of the small angle scattering we have plotted the calculated laboratory angular distributions and data for $\Theta \leqslant 15°$ on a linear scale as shown in Fig. 4. The ESMMSV potential cross section falls essentially on the mLJ-D calculation for the smallest angles while ESMSV-II provides a cross section which consistently lies above the experimental data. Even larger discrepancies occur for the LM potential where the smallest angles for which experimental data are available are in error by 5%. Figure 5 portrays the differences among the potentials most clearly by plotting the deviation between the calculated curves and experimental points as a function of laboratory angle.

In order to demonstrate the precision with which we can determine

the well depth, ε, for this weakly attractive system, we have taken our ESMMSV potential and have performed two additional calculations by taking ε/k = 9.5°K and 11.5°K, representing 10% variations from our best fit value. The small angle scattering for our best fit potential plus these two calculations is plotted on a linear scale with the experimental data in Fig. 6. The difference between experiment and calculation for these extremum potentials is clearly outside of experimental error for $\Theta \leq 8°$. It should be noted that this calculation demonstrates the sensitivity of our data fitting to a particular model for the interatomic potential.

Bickes and Bernstein[29] have recently proposed that the Simons-Parr-Finlan modification[30] of the well known Dunham expansion of the interatomic potential[31] provides a unified representation of multiparameter potential functions used to interpret elastic scattering data at thermal energies. This model expresses the reduced potential function as a power series expansion as follows:

$$f(\lambda) = -1 + b_0\lambda^2\left[1 + \sum_{n=1}^{N} b_n\lambda^n\right]$$

where $\lambda = (r - r_m)/r \equiv 1 - x^{-1}$, with x defined, as usual, as r/r_m.

Bickes and Bernstein have demonstrated that multiparameter potentials recently proposed to fit scattering data can be fitted with a rather small set of coefficients $\{b_i\}$. Accordingly, we have fitted the reduced potential of our proposed He^3-He^4 potential to this modification of the Dunham expansion. We found that an adequate representation of the reduced potential for this system can be achieved with a root-mean-square standard deviation of ± 2% using eight coefficients, i.e., N = 7. As these authors

noted, the spacing of points in the exponential spline region must be increased to achieve a reasonable fit and accordingly, a spacing of 0.04 reduced units was employed in this region. The coefficients providing a best fit to the potential are listed here:

b_0	= 35.9433	b_4	= -79.0467
b_1	= -5.17194	b_5	= 194.977
b_2	= 16.6325	b_6	= 181.106
b_3	= -20.3142	b_7	= -515.087

The potential was fitted to the Dunham expansion over the range $0.68 \leqslant x \leqslant 1.80$. The long range force constant, A_6, in the notation of Bickes and Bernstein, is equal to 1.543.

As a final check and point of comparison among these potentials we have calculated the second virial coefficient as a function of temperature at the lowest temperatures for which experimental data are available. The virial coefficient data are only available for isotopically pure He samples so no conclusion regarding isotope effects in the interatomic potential can be inferred directly. The deviation plots, $B(T)_{calc} - B(T)_{exp}$ vs. T, are shown in Fig. 7. The ESMMSV and mLJ-D potentials provide good overall fits to the data while the ESMSV-II and LM potentials demonstrate negative deviations at the lowest temperatures, indicative of slightly deep wells coupled with outer walls with slightly too much attraction. We have only used B(T) as a diagnostic check on our fit to the scattering data as opposed to varying parameters to optimize the fit to B(T).

Implicit in the above discussion is the fact that no isotope effect is discernable in either the B(T) data or the differential cross section.

The ESMMSV potential derived from He^3-He^4 scattering fits He^4-He^4 B(T) data as well as the mLJ-D potential, extracted from He^4-He^4 scattering data. Furthermore, the ESMMSV potential also provides a good fit to the He^4-He^4 scattering data of ref. 15. Thus, the present data do not appear to support the statement that the He^3-He^4 and He^4-He^4 potentials are measureably different.

The present experimental data provide a more accurate representation of the interaction between two helium atoms and indicate that our knowledge of this system in the region of the attractive minimum has been enhanced over the past three years. It thus appears that the well depth for this system is in the range 10.3 - 10.7°K with r_m between 2.96 and 2.98 Å. The present experimental data provide a more precise value of ϵ than our earlier work primarily because of the greater precision of the data from improved signal-to-noise considerations as opposed ot increased information content from more partial waves in the cross section.

Finally, it is interesting to note that the ESMMSV potential does not support a bound state for He^4-He^4, is in contrast to ESMSV-II which accommodates a bound state for He^4-He^4. Bennewitz et al. have noted that mLJ-D has a bound state, but potentials within their error limits do not. One cannot conclude, at present, that the He-He potential has a bound state.

ACKNOWLEDGMENTS

The authors wish to express their appreciation to Dr. B. Liu and Dr. A. D. McLean for communicating to us their most recent *ab initio* calculation of the He-He potential.

FOOTNOTES AND REFERENCES

*Work performed under the auspices of the U. S. Energy Research and Development Administration.

†Present address: Philips Research Laboratories, N.V. Philips' Gloeilampenfabrieken, Eindhoven, The Netherlands.

‡Present address of J. M. Farrar and Y. T. Lee

1. See, for example, W. H. Keeson, Helium (Elsevier, New York, 1942).
2. J. de Boer and A. Michels, Physica 5, 945 (1938).
3. P. J. Bendt, Phys. Rev. 110, 85 (1958).
4. H. L. Johnston and E. R. Grilly, J. Phys. Chem. 46, 948 (1942).
5. B. B. McInteer, L. T. Aldrich and A. O. Nier, Phys. Rev. 72, 510 (1947).
6. W. W. Watson, A. J. Howard, N. E. Miller and R. M. Schiffrin, Z. Naturforsch. 18a, 242 (1963).
7. D. E. Beck, Mol. Phys. 14, 311 (1968).
8. J. E. Jordan and I. Amdur, J. Chem. Phys. 46, 165 (1967).
9. P. E. Phillipson, Phys. Rev. 125, 1981 (1962).
10. T. L. Gilbert and A. C. Wahl, J. Chem. Phys. 47, 3425 (1967).
11. G. H. Matsumoto, C. F. Bender and E. R. Davidson, J. Chem. Phys. 46, 402 (1967).
12. D. R. McLaughlin and H. F. Schaefer III, Chem. Phys.Lett. 12, 244 (1972).
13. G. Starkschall and R. G. Gordon, J. Chem. Phys. 54, 663 (1971).
14. P. E. Siska, J. M. Parson, T. P. Schafer and Y. T. Lee, J. Chem. Phys. 55, 5762 (1971).
15. J. M. Farrar and Y. T. Lee, J. Chem. Phys. 56, 5801 (1972).
16. P. Cantini, M. G. Dondi, G. Scoles and F. Torello, J. Chem. Phys. 56, 1946 (1972).

17. R. Feltgen, H. Pauly, F. Torello and H. Vehmeyer, Phys. Rev. Lett. 30, 820 (1973).

18. W. H. Miller, J. Chem. Phys. 51, 3631 (1969); 54, 4174 (1971).

19. H. G. Bennewitz, H. Busse, H. D. Dohmann, D. E. Oates and W. Schrader, Z. Physik 253, 435 (1972).

20. H. G. Bennewitz, H. Busse, H. D. Dohmann, D. E. Oates and W. Schrader, Phys. Rev. Lett. 29, 533 (1972).

21. B. Liu and A. D. McLean, to be published.

22. B. Liu, private communication.

23. P. J. Bertoncini and A. C. Wahl, J. Chem. Phys. 58, 1259 (1973).

24. B. Liu and A. D. McLean, J. Chem. Phys. 59, 4557 (1973).

25. P. E. Siska, J. M. Parson, T. P. Schafer, F. P. Tully, Y. C. Wong and Y. T. Lee, Phys. Rev. Lett. 25, 271 (1970).

26. A. Dalgarno and A. L. Stewart, Proc. Roy. Soc. (London) A238, 269 (1956).

27. L. W. Bruch and I. J. McGee, J. Chem. Phys. 52, 5884 (1970).

28. W. D. Davison, Proc. Phys. Soc. (London) 87, 133 (1966).

29. R. W. Bickes, Jr. and R. B. Bernstein, Chem. Phys. Lett. 26, 457 (1974).

30. G. Simons, R. G. Parr and J. M. Finland, J. Chem. Phys. 59, 3229 (1973).

31. J. L. Dunham, Phys. Rev. 41, 721 (1932).

32. J. H. Dymond and E. B. Smith, The Virial Coefficients of Gases: A Critical Compilation (Clarendon, Oxford, 1969).

33. W. E. Keller, Phys. Rev. 97, 1 (1955).

34. W. H. Keesom and W. K. Walstra, Comm. Leiden, No. 260C (1940); Physica 7, 985 (1940).

35. Dr. R. Gengenbach kindly informed us that ESMSV-II does accommodate a bound state.

FIGURE CAPTIONS

Fig. 1. (a) He^3-He^4 lab angular distribution. Calculated curve from ESMMSV potential discussed in this work. Error bars on data points of He^3 denote one standard deviation.
(b) He^4-He^4 lab angular distribution (ref. 15) with ESMMSV calculation (——) and ESMSV-II calculation (----) of ref. 15.

Fig. 2. He-He potential functions.

Fig. 3. He^3-He^4 laboratory elastic scattering cross sections calculated with four potentials: ESMMSV (this work), MLJ-D (ref. 19), LM (ref. 21), and ESMSV-II (ref. 15).

Fig. 4. Small angle scattering for four potentials of Fig. 3. Note linear scale.

Fig. 5. $[I(\Theta)_{calc} - I(\Theta)_{exp}]/I(\Theta)_{exp}$ vs. Θ for four potentials of Fig. 3. Error bars denote one standard deviation of data points.

Fig. 6. Small angle scattering for 10% variations in ϵ about the best fit value for ESMMSV. Experimental data shown for comparison.

Fig. 7. Second virial coefficient deviation plot, $B(T)_{calc} - B(T)_{exp}$ vs. T for He^4-He^4 data. Calculations for four model potentials as shown in the text. Data: (O), ref. 32; (●), ref. 33; (Δ), ref. 34, and (■), ref. 1.

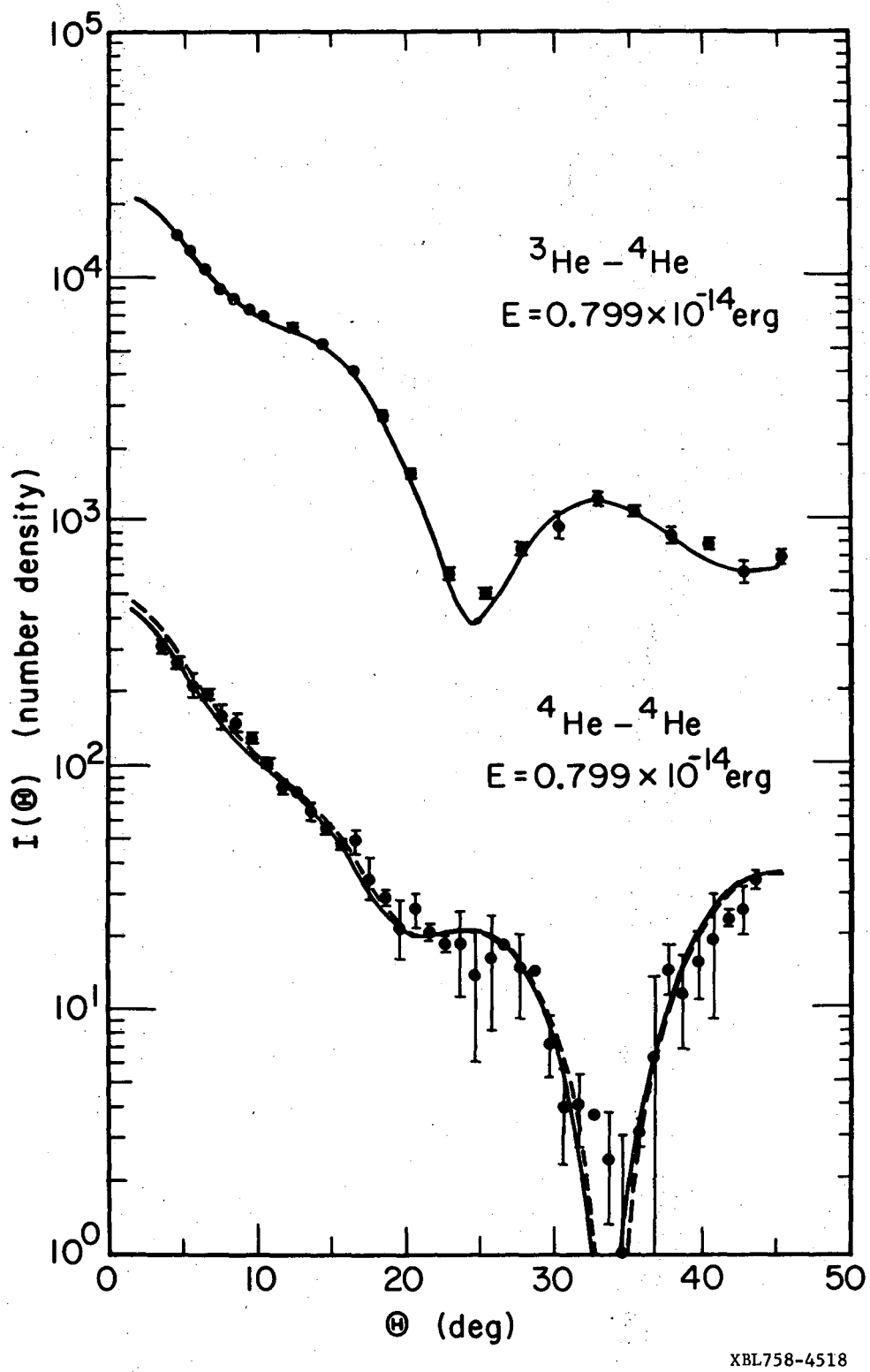

Fig. 1

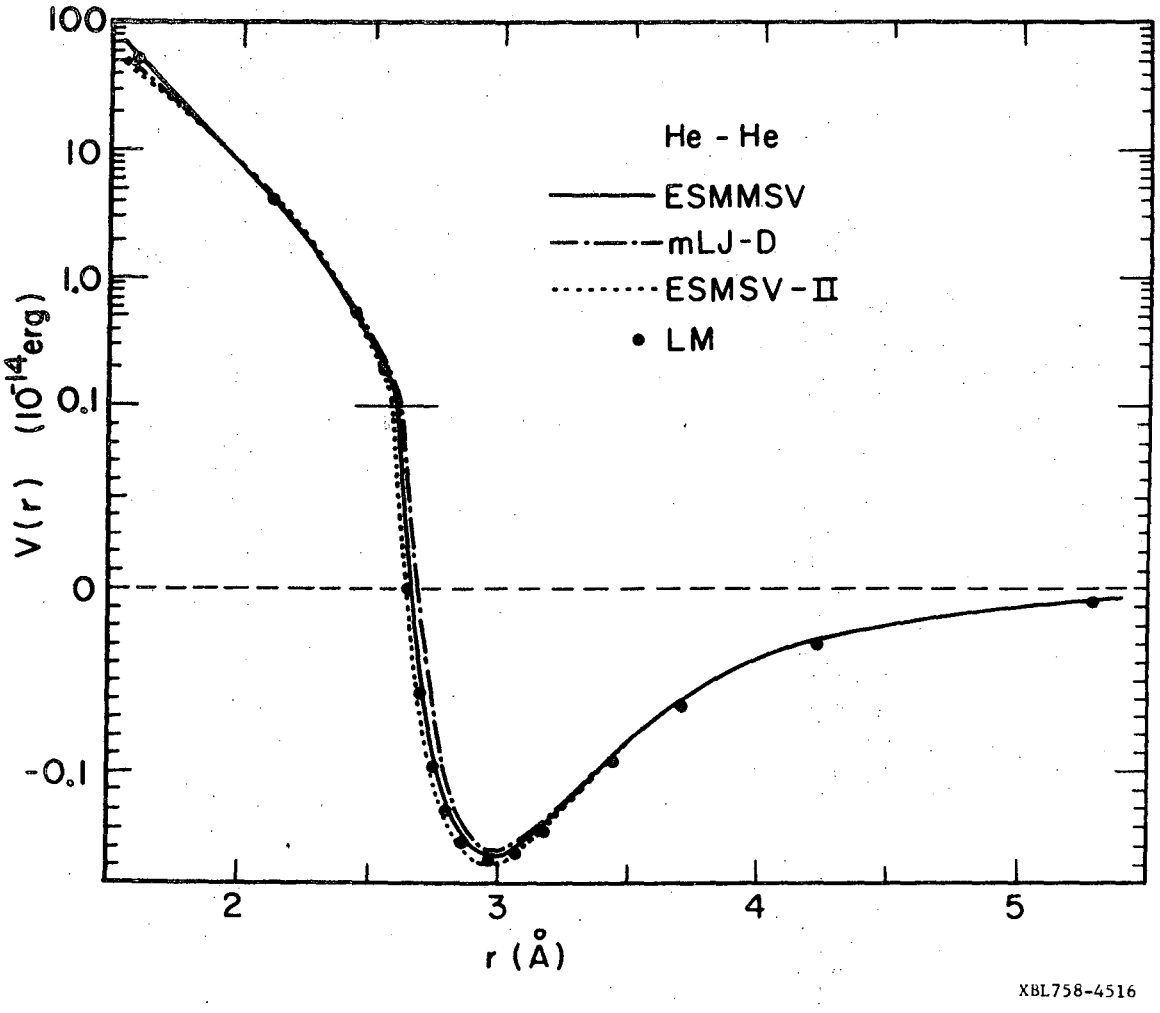
100
10
1.0
0.1
0
-0.1
V(r) (10^{-14}erg)
2
3
4
5
r (Å)
He - He
ESMMSV
mLJ-D
ESMSV-II
LM
XBL758-4516

Fig. 2

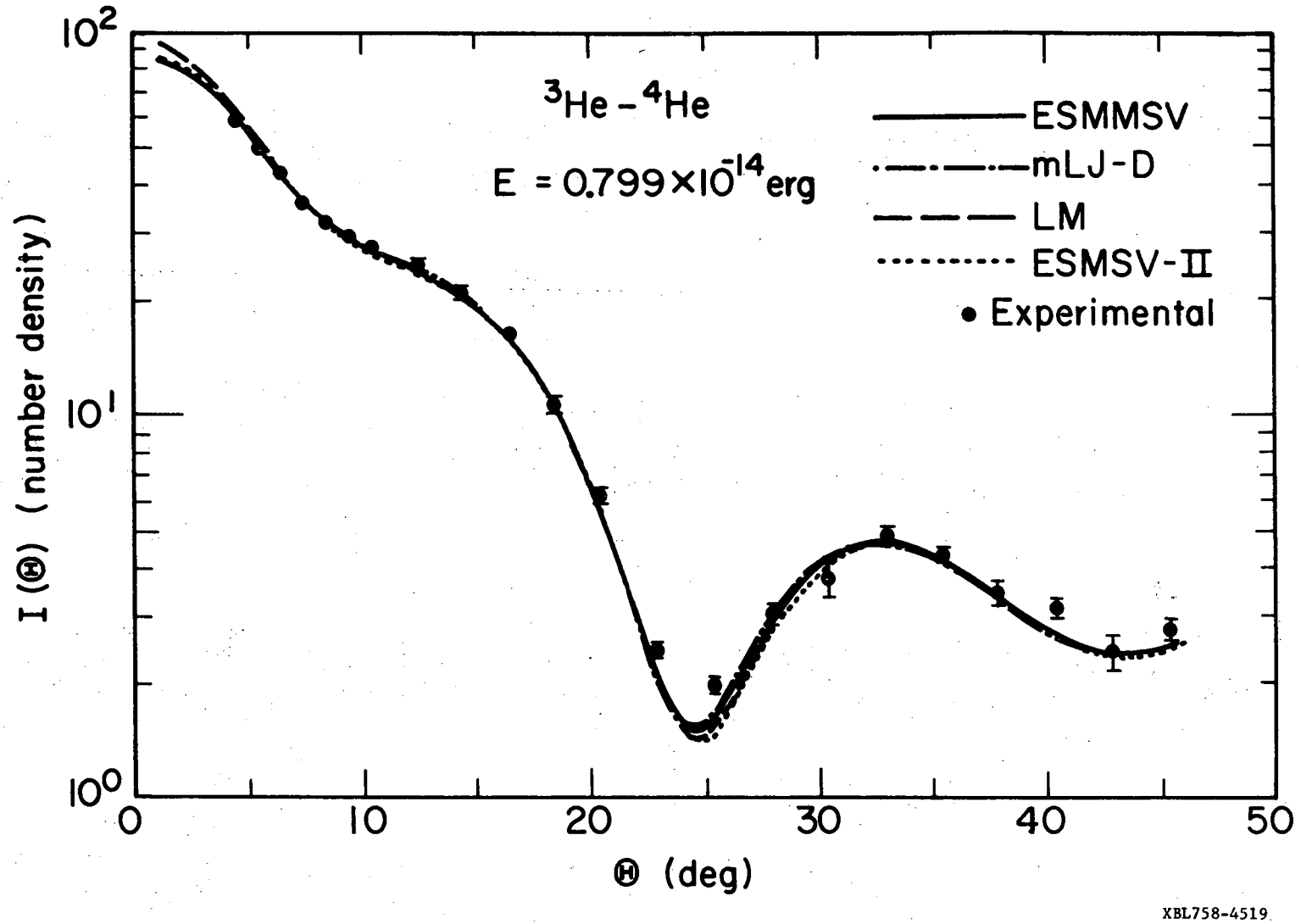

Fig. 3

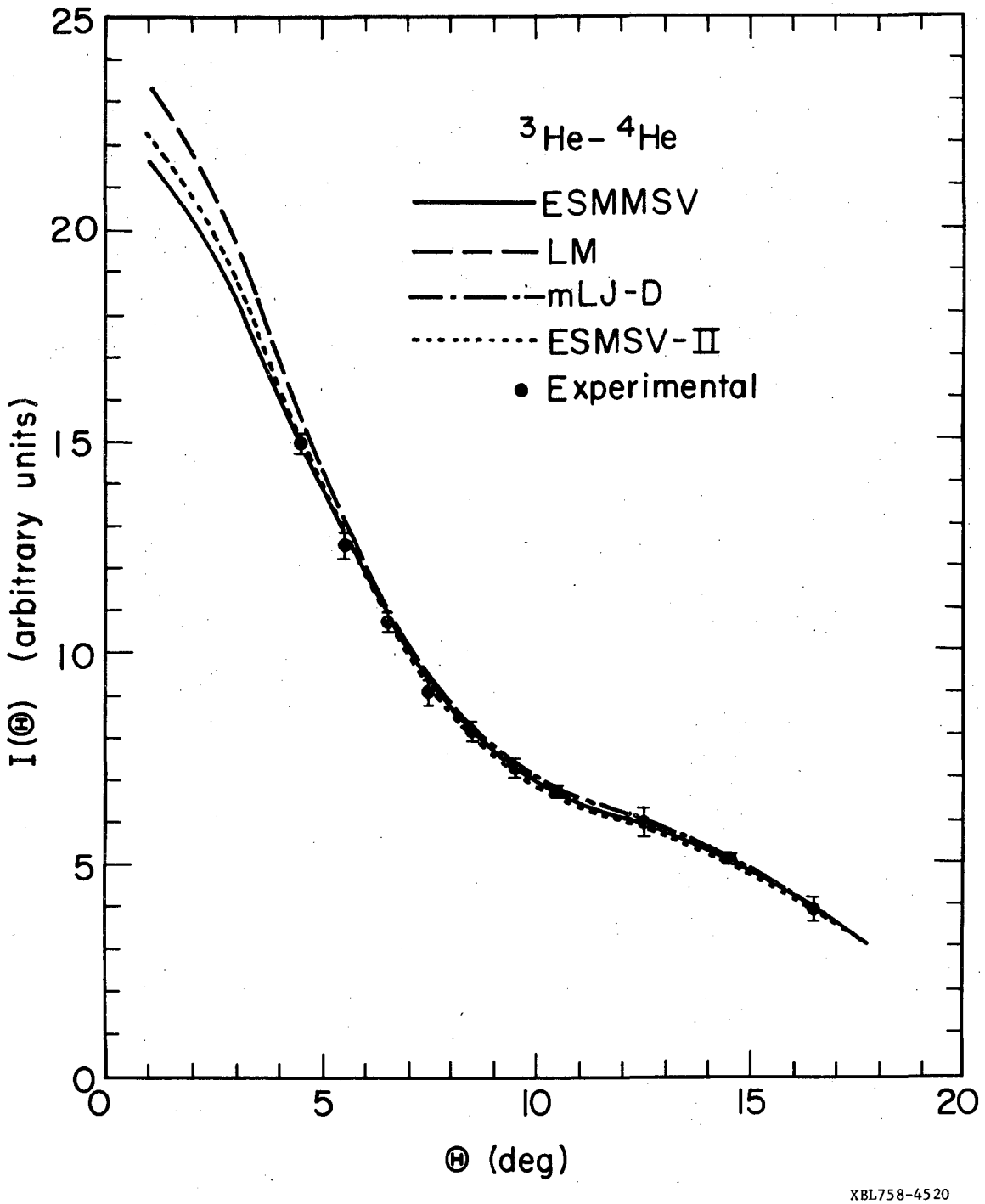
^{3}He - ^{4}He
ESMMSV
LM
mLJ-D
ESMSV-II
Experimental
I(Θ) (arbitrary units)
Θ (deg)
0
5
10
15
20
25
XBL758-4520

Fig. 4

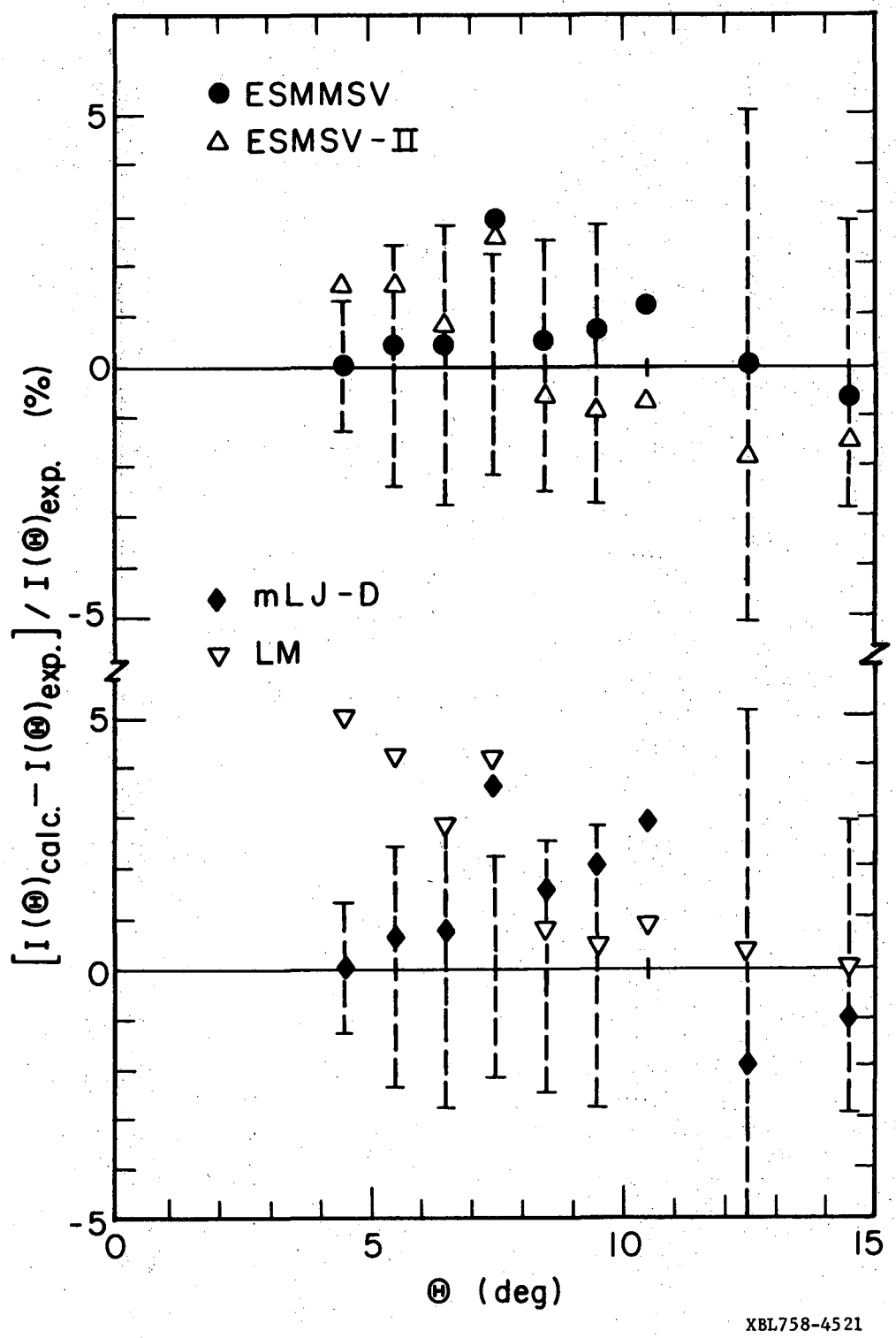
ESMMSV
ESMSV-II
mLJ-D
LM
5
0
-5
5
0
-5
0
5
10
15
Θ (deg)
[I(Θ)calc.− I(Θ)exp.] / I(Θ)exp. (%)
XBL758-4521

Fig. 5

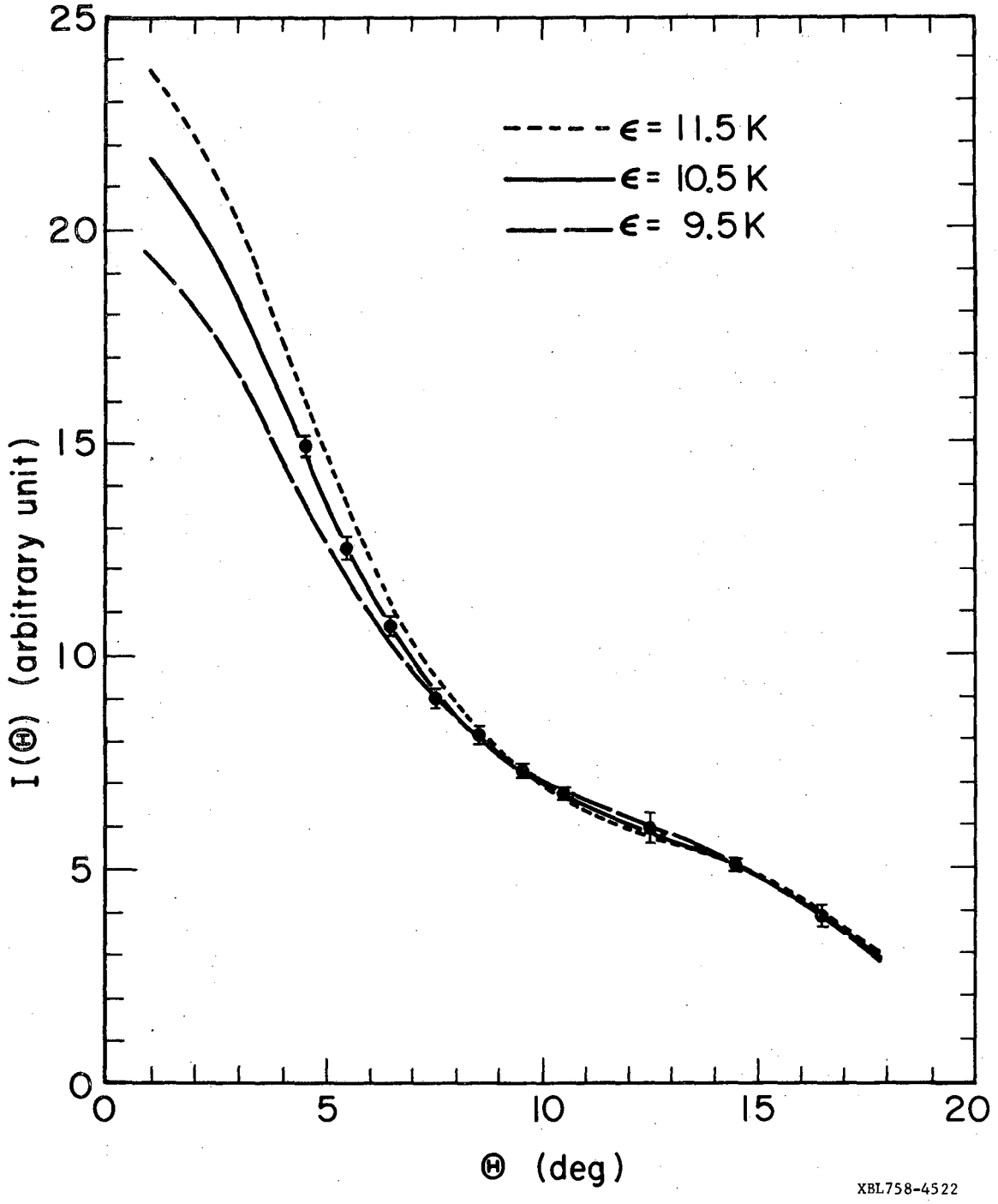
25
20
15
10
5
0
0
5
10
15
20
I(Θ) (arbitrary unit)
Θ (deg)
ϵ = 11.5 K
ϵ = 10.5 K
ϵ = 9.5 K
XBL758-4522

Fig. 6

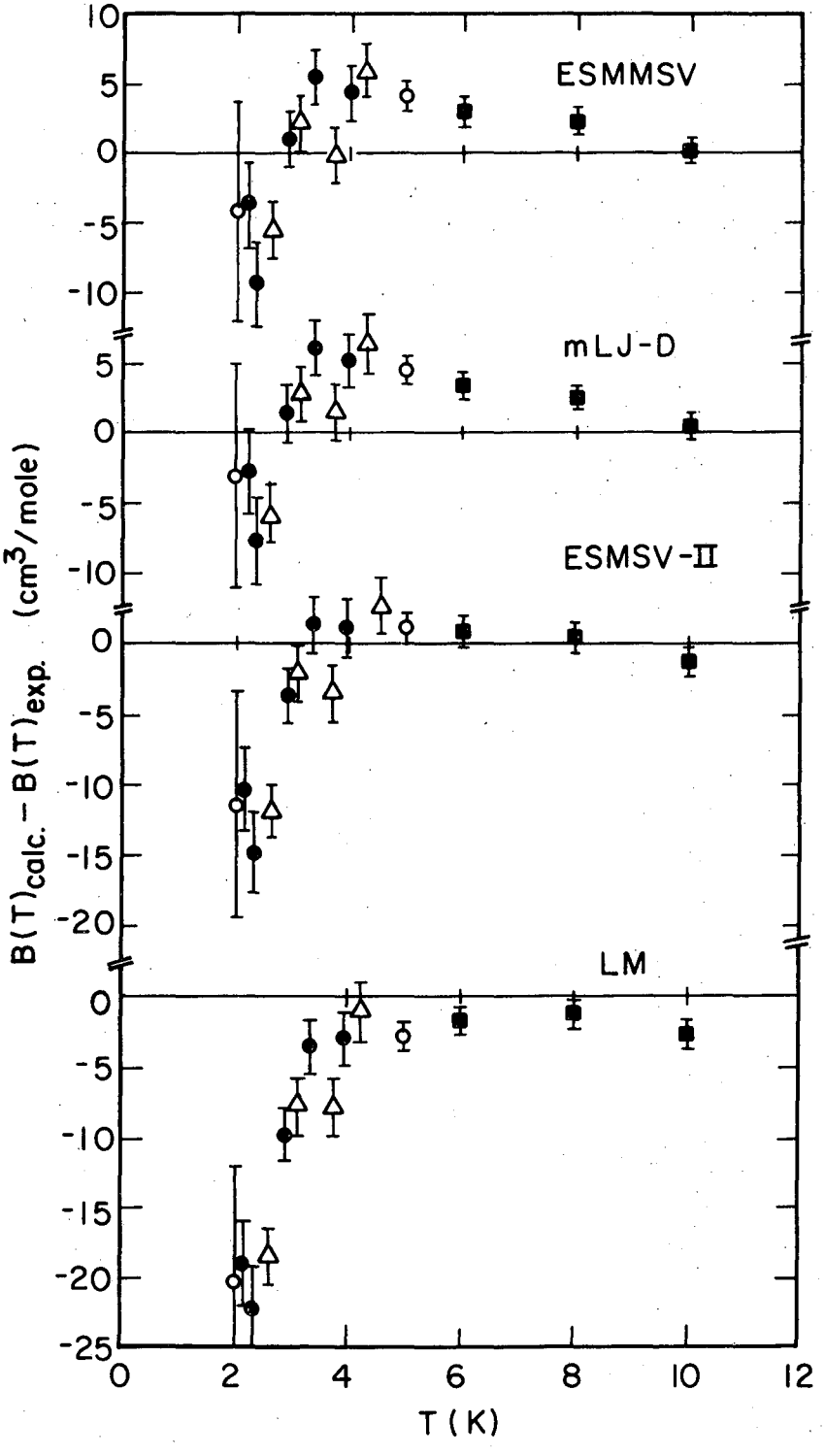

Fig. 7

TECHNICAL INFORMATION DIVISION
LAWRENCE BERKELEY LABORATORY
UNIVERSITY OF CALIFORNIA
BERKELEY, CALIFORNIA 94720